

Active optical clock based on four-level quantum system

ZHANG TongGang*, WANG YanFei, ZANG XiaoRun, ZHUANG Wei & CHEN JingBiao

State Key Laboratory of Advanced Optical Communication Systems and Networks, Institute of Quantum Electronics, School of Electronics Engineering & Computer Science, Peking University, Beijing 100871, China

Received July 5, 2012; accepted November 28, 2012

Active optical clock, a new conception of atomic clock, has been proposed recently. In this work, we propose a scheme of active optical clock based on four-level quantum system. The final accuracy and stability of two-level quantum system are limited by second-order Doppler shift of thermal atomic beam. To three-level quantum system, they are mainly limited by light shift of pumping laser field. These limitations can be avoided effectively by applying the scheme proposed here. Rubidium atom four-level quantum system, as a typical example, is discussed. The population inversion between $6S_{1/2}$ and $5P_{3/2}$ states can be built up at a time scale of 10^{-6} s. With the mechanism of active optical clock, in which the cavity mode linewidth is much wider than that of the laser gain profile, it can output a laser with quantum-limited linewidth narrower than 1 Hz in theory. An experimental configuration is designed to realize this active optical clock.

active optical clock, population inversion, narrow linewidth, light shift

Citation: Zhang T G, Wang Y F, Zang X R, et al. Active optical clock based on four-level quantum system. *Chin Sci Bull*, 2013, 58: 2033–2038, doi: 10.1007/s11434-013-5877-0

Optical clocks have demonstrated great improvements in stability and accuracy over the microwave frequency standards. Since the proposal of active optical clock [1–3], a number of neutral atoms with two-level, three-level and four-level at thermal beam, laser cooling and trapping configurations have been investigated recently [1–14]. The potential quantum-limited linewidth of active optical clock is narrower than mHz, and it is possible to reach this unprecedented linewidth since the thermal noise of cavity mode can be reduced dramatically with the mechanism of active optical clock. It has been recognized that active optical clock has the potential to improve the stability of the best atomic clocks by about 2 orders of magnitude [9, 10, 15].

Until now, the major experimental schemes of active optical clock are based on trapped quantum system and atomic beam quantum system. To the latter, the residual Doppler shift will be the main limitation, thus the final accuracy and stability of two-level quantum system are limited by second-order Doppler shift of thermal atomic beam. Laser

cooled and trapped quantum system provides a solution to this limitation. As for three-level quantum system, the system stability and accuracy are mainly affected by the light shift of pumping laser. Four-level quantum system can overcome these limitations and thus will be a better choice for active optical clock with improved performance [6].

Rubidium, as one of alkali metals, has been investigated as the critical research atom of Bose-Einstein condensate, photonic Josephson effect, fractionalized vortices in lattice due to the mature technique of laser cooling and trapping [16–18].

We have investigated several alkali metals including potassium, rubidium and cesium and found that the four-level quantum systems of these elements are appropriate choices based on the mechanism of active optical clock. Here we take rubidium atom as an example. The population inversion can be realized as shown in Figure 1.

A 421.7 nm laser operating at $5S_{1/2}$ to $6P_{1/2}$ transition is used as pumping laser. First, the atoms at $5S_{1/2}$ state are pumped to $6P_{1/2}$ state, and then decay to $5S_{1/2}$, $6S_{1/2}$ and $4D_{3/2}$ states by spontaneous transitions. Second, the atoms at $6S_{1/2}$ and $4D_{3/2}$ states decay to $5P_{1/2}$ and $5P_{3/2}$ states

*Corresponding author (email: ztg@pku.edu.cn)

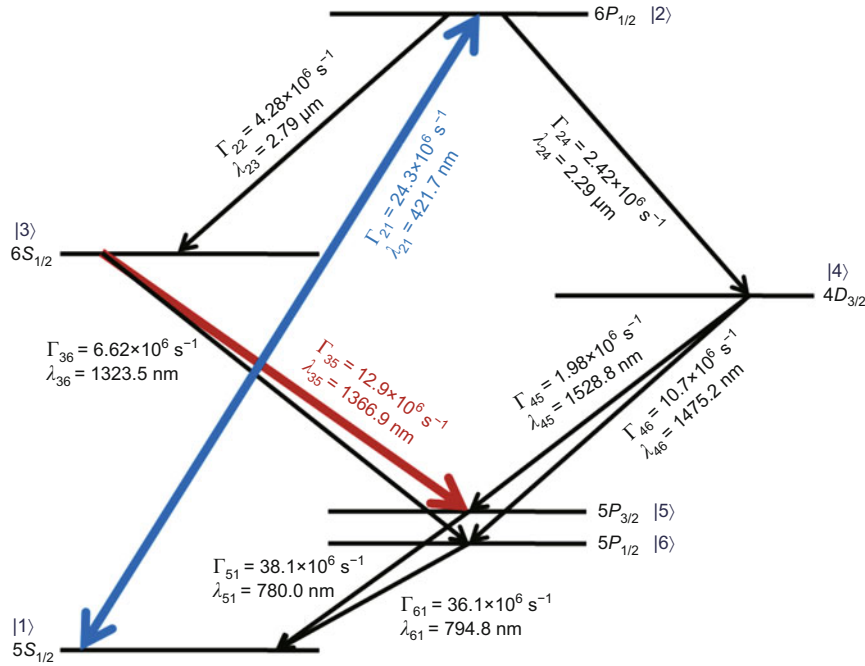


Figure 1 (Color online) Scheme of Rb four-level quantum system active optical clock operating at 1366.9 nm clock transition, pumped with 421.7 nm laser.

respectively. Third, the atoms at $5P_{1/2}$ and $5P_{3/2}$ states return to ground state $5S_{1/2}$ and then are pumped to $6P_{1/2}$ state by pumping laser again. This process continues until the population inversion is established between $6S_{1/2}$ and $5P_{3/2}$ states since the lifetime of $6S$ state is longer than that of $5P$ state.

One should note that the population inversions are also built up between $6S_{1/2}$ – $5P_{1/2}$, $4D_{3/2}$ – $5P_{3/2}$ and $4D_{3/2}$ – $5P_{1/2}$ states. We choose $6S_{1/2}$ and $5P_{3/2}$ states as the object of study in this paper because the population inversion between them is the greatest according to our calculation. At the same time, one should pay attention to the fact that the split of the two hyperfine levels of $5P_{1/2}$ state is wider than that of $5P_{3/2}$ state. So if we want to realize this active optical clock in experiment, the transition between $6S_{1/2}$ and $5P_{1/2}$ states will be a better selection for avoiding modes competition.

Once the population inversion is built up, a Fabry-Perot type resonator, with a bad cavity whose cavity mode linewidth is much wider than that of the laser gain profile, is used to realize active optical clock laser output. Using the definition of $a = \Gamma_c/\Gamma_{\text{gain}}$ [1, 2, 19], here Γ_c is cavity loss rate and Γ_{gain} is gain medium linewidth. According to the mechanism of active optical clock [1], the Fabry-Perot resonator should be pushed deep down into the bad-cavity regime $a \gg 1$. The quantum-limited linewidth of active optical clock based on four-level quantum system is expected to be narrower than Hz.

In this work, we will present the result of the calculations of dynamical process of population inversion, and lasing process with a bad cavity. An experimental scheme is designed to realize Rb four-level quantum system active optical clock.

1 Population inversion of Rubidium atoms four-level quantum system

A pumping laser operating at 421.7 nm is used to realize population inversion of Rb four-level quantum system. The Rabi frequency of pumping laser is $\Omega = d \cdot \varepsilon/\hbar$, where d is electric dipole matrix between $5S_{1/2}$ state and $6P_{1/2}$ state, ε is electric field strength of the pumping laser. The spontaneous decay rate is $\Gamma_{21} = \omega_{21}^3 d^2 / (3\pi\hbar c^3 \varepsilon_0)$ where $\omega_{21} = 2\pi c/\lambda_{21}$. The relationship between light intensity of pumping laser and the Rabi frequency is $I = 2\pi\hbar c \Omega^2 / (3\lambda_{21}^3 \Gamma_{21})$. If the pumping laser is 10 mW with beam waist 1 mm, and considering that $\Gamma_{21} = 2.43$ MHz, the pumping rate from $5S_{1/2}$ to $6P_{1/2}$ is $\Omega = 3.7 \times 10^7 \text{ s}^{-1}$. The saturation light intensity is $I_s = \pi\hbar c \Gamma_{21} / (3\lambda_{21}^3) = 0.7 \text{ mW/cm}^2$, and $\Omega_s = 1.7 \times 10^6 \text{ s}^{-1}$ for $I = I_s$. So the Rabi frequency Ω can be set from $1.7 \times 10^6 \text{ s}^{-1}$ to about $3.7 \times 10^7 \text{ s}^{-1}$.

Supposing that atoms are within a thermal gas cell or magneto-optical trap (MOT), part of the atoms would be pumped to $6P_{1/2}$ state. Atoms at $6P_{1/2}$ state spontaneously decay to metastable states $6S_{1/2}$ and $4D_{3/2}$ and continue decaying to the lower state. The atoms that return to $5S_{1/2}$ state are repumped by the pumping laser. When the 421.7 nm pumping laser is operating on one of the two hyperfine structure energy levels of $5S$ ground state, a repumping laser can be added to close the atoms leakage to the other hyperfine structure energy level. We will not discuss the repumping laser function in this paper for simplicity. Finally, the population inversion could be established between $6S_{1/2}$ and $5P_{3/2}$ states. The whole process is clear after an approximate calculation in the following.

The density matrix equations for Rb atoms in a thermal gas cell interaction with the pumping light, based on the theories of interaction between atoms and light, are written in RWA-approximation as follows:

$$\begin{aligned}
 \frac{d\rho_{11}}{dt} &= -\Omega\rho_{12}^I + \Gamma_{21}\rho_{22} + \Gamma_{51}\rho_{55} + \Gamma_{61}\rho_{66}, \\
 \frac{d\rho_{22}}{dt} &= \Omega\rho_{12}^I - (\Gamma_{21} + \Gamma_{23} + \Gamma_{24})\rho_{22}, \\
 \frac{d\rho_{33}}{dt} &= \Gamma_{23}\rho_{22} - (\Gamma_{35} + \Gamma_{36})\rho_{33}, \\
 \frac{d\rho_{44}}{dt} &= \Gamma_{24}\rho_{22} - (\Gamma_{45} + \Gamma_{46})\rho_{44}, \\
 \frac{d\rho_{55}}{dt} &= \Gamma_{35}\rho_{33} + \Gamma_{45}\rho_{44} - \Gamma_{51}\rho_{55}, \\
 \frac{d\rho_{66}}{dt} &= \Gamma_{36}\rho_{33} + \Gamma_{46}\rho_{44} - \Gamma_{61}\rho_{66}, \\
 \frac{d\rho_{12}^I}{dt} &= \frac{1}{2}\Omega(\rho_{11} - \rho_{22}) + \rho_{12}^R\Delta - \frac{1}{2}\Gamma_{21}\rho_{12}^I, \\
 \frac{d\rho_{12}^R}{dt} &= -\rho_{12}^I\Delta - \frac{1}{2}\Gamma_{21}\rho_{12}^R.
 \end{aligned} \quad (1)$$

The subscript numbers of the density matrix correspond to different energy levels shown in Figure 1. The diagonal elements ρ_{11} , ρ_{22} and so on mean the probability of atoms in corresponding states. ρ_{12}^R means energy shift and ρ_{12}^I means power broadening. $\Delta = \omega_{21} - \omega$ is frequency detuning of pumping light on the transition frequency and can be set to 0. Γ_{21} and Γ_{23} are decaying rates related to the lifetimes of corresponding energy levels described in Figure 1.

The numerical solutions of the above equations are shown in Figure 2. It is obvious that under the action of pumping laser, the atoms at $5S_{1/2}$ state decrease rapidly. The oscillation of ρ_{11} and ρ_{22} is caused by the assumption that the 421.7 nm pumping laser is monochromatic. At steady-state, the value of ρ_{33} is 8.4% and ρ_{55} is 3.3%. This means the atoms in $6S_{1/2}$ state are about 2.5 times as many as that in $5P_{3/2}$ state, therefore the population inversion is built up. From Figure 2 we can also conclude that the population inversion between $6S_{1/2}$ and $5P_{3/2}$ states is built up at a time scale of 10^{-6} s. Other population inversions between $6S_{1/2}$ - $5P_{1/2}$, $4D_{3/2}$ - $5P_{3/2}$ and $4D_{3/2}$ - $5P_{1/2}$ states are established simultaneously. We can experimentally detect the fluorescence spectrum and

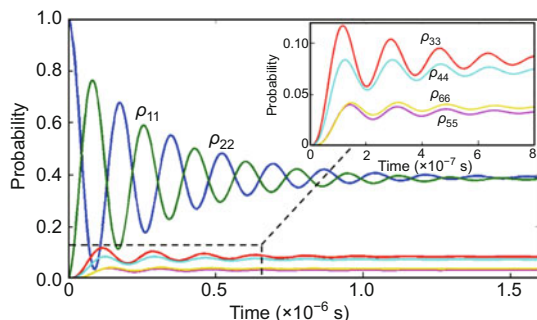


Figure 2 (Color online) The dynamical populations of Rb atom with Rabi frequency $\Omega = 1.8 \times 10^7 \text{ s}^{-1}$.

calculate relative lines intensity to demonstrate whether these population inversions are built up.

2 Lasing of Rubidium four-level quantum system active optical clock

An optical resonant cavity could be applied to detect the probability of lasing transition between the inverted states $6S_{1/2}$ and $5P_{3/2}$ as the population inversion occurs. According to the classical laser theory, the oscillating process could start up once the optical gain exceeding the loss rate. Here we use a bad cavity ($\Gamma_c \gg \Gamma_{\text{gain}}$) to realize laser output. When the stimulated radiation starts and reaches the condition of self-oscillation, the laser oscillation is built up and then output the 1366.9 nm laser of active optical clock which will be used as laser frequency standards.

The atom-cavity coupling constant g [20, 21] is given as $g = \sqrt{\mu^2\omega_{35}/(2\hbar\epsilon_0V_{\text{mode}})}$, where $\omega_{35} = 2\pi c/\lambda_{35}$ and $\mu^2 = 3\pi\hbar c^3\epsilon_0\Gamma_{35}/\omega_{35}^3$. Then the atom-cavity coupling constant g can be written as $g^2 = 3c\Gamma_{35}\lambda_{35}^2/(8\pi V_{\text{mode}})$. The variation range of g is about from $3 \times 10^4 \text{ s}^{-1}$ to $9 \times 10^5 \text{ s}^{-1}$ for reasonable value of V_{mode} . The laser emission coefficient is $\sin^2(\sqrt{n+1}g\tau_{\text{int}})$ [20, 21], where $\tau_{\text{int}} = 1/(\Gamma_3 + \Gamma_5) = 17.4 \text{ ns}$ considering the condition of $\sqrt{n+1}g\tau_{\text{int}} \geq \pi/2$ in our case discussed here. Define the cycle time for Rb atoms through the passage of $5S_{1/2}$, $6P_{1/2}$, $6S_{1/2}$ and $5P_{3/2}$ states with the action of 421.7 nm pumping laser during transition time as

$$\tau_{\text{cyc}} = \frac{1}{\Gamma_2} + \frac{1}{\Gamma_3} + \frac{1}{\Gamma_5} + \frac{1}{\Omega} \quad (2)$$

and $\tau_{\text{cyc}} = 225 \text{ ns}$ for $\Omega = 2.64 \times 10^7 \text{ s}^{-1}$ neglecting other channel. Thus the inverted atoms that are possible to emit photons per unit time is $(\rho'_{33} - \rho'_{55})/\tau_{\text{cyc}}$, where ρ'_{33} and ρ'_{55} represent the number of atoms in $6S_{1/2}$ state and $5P_{3/2}$ state. So the gain term of the rate equation for cavity photon number n is $\sin^2(\sqrt{n+1}g\tau_{\text{int}})(\rho'_{33} - \rho'_{55})/\tau_{\text{cyc}}$.

The equations for emitted photons (n) from the total atoms inside the cavity mode (N), together with corresponding density matrix equations are listed as follows. Here we apply the form of semiclassical approximation of four-level quantum system [20, 21], then

$$\begin{aligned}
 \frac{d\rho'_{11}}{dt} &= -\Omega\rho'_{12} + \Gamma_{21}\rho'_{22} + \Gamma_{51}\rho'_{55} + \Gamma_{61}\rho'_{66}, \\
 \frac{d\rho'_{22}}{dt} &= \Omega\rho'_{12} - (\Gamma_{21} + \Gamma_{23} + \Gamma_{24})\rho'_{22}, \\
 \frac{d\rho'_{33}}{dt} &= \Gamma_{23}\rho'_{22} - (\Gamma_{35} + \Gamma_{36})\rho'_{33} \\
 &\quad - \frac{\rho'_{33} - \rho'_{55}}{\tau_{\text{cyc}}} \sin^2(\sqrt{n+1}g\tau_{\text{int}}), \\
 \frac{d\rho'_{44}}{dt} &= \Gamma_{24}\rho'_{22} - (\Gamma_{45} + \Gamma_{46})\rho'_{44}, \\
 \frac{d\rho'_{55}}{dt} &= \Gamma_{35}\rho'_{33} + \Gamma_{45}\rho'_{44} - \Gamma_{51}\rho'_{55}
 \end{aligned}$$

$$\begin{aligned}
& + \frac{\rho'_{33} - \rho'_{55'}}{\tau_{\text{cyc}}} \sin^2(\sqrt{n+1}g\tau_{\text{int}}), \\
\frac{d\rho'_{66}}{dt} &= \Gamma_{36}\rho'_{33} + \Gamma_{46}\rho'_{44} - \Gamma_{61}\rho'_{66}, \\
\frac{d\rho'_{12}}{dt} &= \frac{1}{2}\Omega(\rho'_{11} - \rho'_{22}) + \rho_{12}^R\Delta - \frac{1}{2}\Gamma_{21}\rho'_{12}, \\
\frac{d\rho_{12}^R}{dt} &= -\rho'_{12}\Delta - \frac{1}{2}\Gamma_{21}\rho_{12}^R, \\
\frac{dn}{dt} &= \frac{\rho'_{33} - \rho'_{55'}}{\tau_{\text{cyc}}} \sin^2(\sqrt{n+1}g\tau_{\text{int}}) - \Gamma_c n. \quad (3)
\end{aligned}$$

One should note that the variables ρ'_{11} in these equations, which represent the number of atoms in the corresponding states, are different from those in eq. (1). At room temperature the number of Rb atoms in the cavity mode is about $N = 7 \times 10^9$ with $V_{\text{mode}} = 10^{-7} \text{ m}^3$. N can be changed through the adjustment of temperature and V_{mode} . At 120°C , there are about 2×10^{12} atoms inside the cavity mode with the same mode volume. $\rho'_{11} = N$ and others are all 0 at the beginning. The cavity loss rate $\Gamma_c = a\Gamma_{\text{gain}}$, where $\Gamma_{\text{gain}} = \Gamma_{sp}$ is the natural linewidth of clock transition for laser cooled atoms in MOT, and Γ_{sp} equals to 12.9 MHz here. For atoms in thermal gas cell, we assume the coherent 421.7 nm pumping laser only pumps atoms with velocity near zero for simplicity, then the $\Gamma_{\text{gain}} \approx \Gamma_{sp}$ holds approximately. To reduce the effect caused by the thermal noise of cavity, the cavity loss rate Γ_c should be far greater than the natural linewidth of output laser (Γ_{35}). We set $a = 100$ in this paper.

Figure 3 describes the solutions for the photon number equation. The steady-state value of photon number \bar{n} decrease with the enhancement of atom-cavity coupling constant. The increase of total atoms inside the cavity mode has less influence over \bar{n} compared to the variation of g . Figure 4 describes the dynamical lasing process with the action of pumping laser. We can conclude that a stable laser field is built up within laser cavity on condition that the population inversion is preserved. The steady-state photon number $\bar{n} = 3.76 \times 10^6$ for $g = 9 \times 10^4 \text{ s}^{-1}$ ($V_{\text{mode}} = 10^{-7} \text{ m}^3$) and $N = 2 \times 10^{12}$. The corresponding output laser power

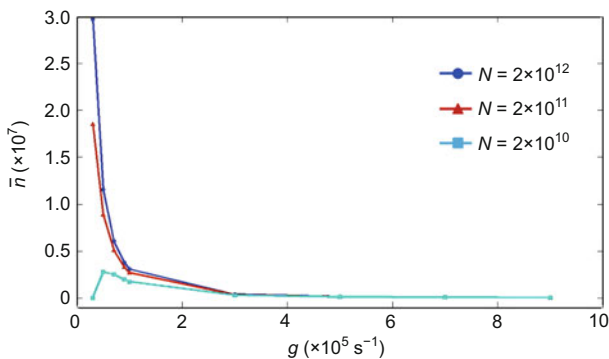


Figure 3 (Color online) The photon number at steady-state inside the cavity varies with the atom-cavity coupling constant g under different value of N .

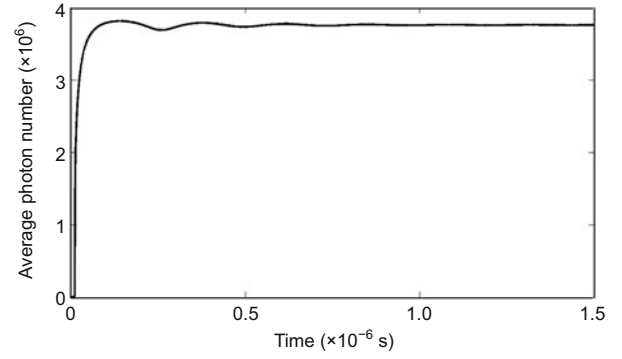


Figure 4 The average photon number inside the cavity under the condition of $\Omega = 2.64 \times 10^7 \text{ s}^{-1}$, $g = 9 \times 10^4 \text{ s}^{-1}$ and $N = 2 \times 10^{12}$.

$P = \bar{n}h\nu_{35}\Gamma_c$ is 0.7 mW.

Since $\Gamma_3, \Gamma_5, \Gamma_{35} < \tau_{\text{int}}^{-1} \ll \Gamma_c$, the quantum linewidth of the active optical clock can be approximated to be $D = g^2/\Gamma_c$ [7]. Therefore we can get the quantum-limited linewidth of Rb four-level quantum system active optical clock in the magnitude of Hz level. If $g = 3 \times 10^4 \text{ s}^{-1}$ and $\Gamma_c = 1.29 \times 10^9 \text{ s}^{-1}$, the linewidth is 0.7 Hz.

In consideration of the fact that the 421.7 nm pumping laser is far detuning from the 1366.9 nm clock transition laser, the light shift of $6S_{1/2} - 5P_{3/2}$ clock transition caused by the 421.7 nm pumping laser can be written as Ω^2/Δ' , where Δ' is the detuning which equals $3.77 \times 10^{15} \text{ Hz}$. Given the Rabi frequency $\Omega = 2.64 \times 10^7 \text{ s}^{-1}$, the light shift will be 0.18 Hz. The stability of 421.7 nm pumping laser power can be better than 10^{-3} , therefore the uncertainty of light shift due to pumping laser is less than 0.18 mHz. This means to four-level quantum system, the influence on system stability and accuracy induced by light shift is far less than that of two-level and three-level quantum systems. Considering the mature technology of laser cooling and trapping of Rb atoms, one can establish a 421.7 nm Rb MOT directly for Rb active optical clock, and the cooling and trapping laser will play the pumping role also since its light shift is small enough.

3 Experimental design of active optical frequency standards based on Rubidium four-level quantum system

The lasing of Rb four-level quantum system active optical clock can be realized by using a conventional Fabry-Perot resonator. But the difference is that the cavity loss rate Γ_c far outweighs the natural linewidth Γ_{sp} .

The length of this cavity L is set to 1.5 cm, then the free spectral range is $FSR = c/(2L) = 10 \text{ GHz}$. The fineness

$$F = \frac{FSR}{\Gamma_c} = \frac{\pi\sqrt{r_1 r_2}}{1 - r_1 r_2} = \frac{\pi\sqrt{R}}{1 - R}, \quad (4)$$

where $R = r_1 r_2$. Given $\Gamma_c = 1.29 \text{ GHz}$, from above equation we can get $F = 7.75$. Thus we can determine $R = 0.67$,

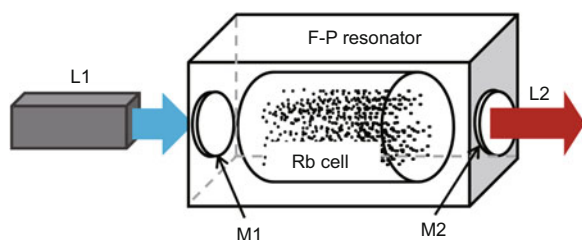


Figure 5 (Color online) The experimental configuration of Rb four-level quantum system active optical clock. L1 is the 421.7 nm pumping laser source. L2 is the 1366.9 nm output clock transition laser. M1 and M2 are coated mirrors.

$r_1 = 1$ and $r_2 = 0.67$. M1 mirror is coated with 421.7 nm anti-reflection coating and 1366.9 nm high-reflection coating. M2 mirror is coated with 421.7 nm high-reflection coating and the reflectivity of 1366.9 nm is 67%. The final output laser comes out from M2. Compared with other optical clock schemes, there are two interesting points of this experimental scheme. The first one is that the most parameters of atomic structure of alkali metals including Rb have been measured precisely already. The second one is that the laser cooling and trapping technology of alkali metals including Rb is currently very mature, thus the thermal gas cell can be replaced by magneto-optical trap for reducing the influence of Doppler effect. The center frequency of four-level quantum system active optical clock is decided by the transition frequency of Rb atoms, but not the laser cavity mode which is very sensitive to the vibration and fluctuation of temperature. The cavity mode of active optical clock can be locked to a reference cavity with low thermal noise [22], then the cavity pulling reduced by a factor of $a = \Gamma_c / \Gamma_{\text{gain}}$ will be smaller than mHz.

4 Discussion and conclusion

Active optical clock, whose quantum-limited linewidth of output laser is far narrower than the natural linewidth of atomic spectrum and its center frequency is not directly subject to cavity mode noise, can provide optical frequency standards with high stability and accuracy. Considering the accuracy requirement, lasing of a three-level conventional laser is not so suitable for an active optical frequency standards because the light shift due to the high intensity pumping laser cannot be tolerable. Thus it needs special design of pumping scheme for active optical clock with three-level configuration [2, 9].

Four-level quantum system active optical frequency standards not only possesses the advantages of active clock such as narrow linewidth and high stability and accuracy, but also overcomes the limitation on stability and accuracy due to light shift. Rb atom four-level quantum system, as a typical example, is studied in detail. Other alkali metals including potassium and cesium have similar four-level quantum systems structures and therefore are appropriate candidates for this novel scheme of active optical clock. The parameters of

atomic structure of these atoms have been measured precisely already thus provides great convenience. Take cesium as an example, the levels $6S_{1/2}$, $7P_{3/2}$, $7S_{1/2}$ and $6P_{3/2}$ compose a four-level quantum system suitable for active optical frequency standards. Population inversion in cesium atoms has been achieved in our preliminary experiment. It is expected to realize active optical clock based on four-level quantum system in our next experimental study.

We mainly study atoms in thermal gas cell in this paper. It is valuable to notice that four-level quantum system based on atoms in MOT can reduce the influence of Doppler effect greatly. To reduce the effect of collision shift and decrease Doppler effect further, magic wavelength lattice trapped atoms can be applied. Besides, laser cooling and trapping technology of alkali metals is very mature. So active optical lattice clock based on four-level quantum system atoms is expected to greatly improve the properties of atomic clocks.

In summary, we propose a scheme of four-level quantum system active optical clock with Rb atoms. Our calculations show that the population inversion between $6S_{1/2}$ and $5P_{3/2}$ states of Rb atom can be built up at a time scale of 10^{-6} s. With 421.7 nm pumping laser operating at $5S_{1/2}$ to $6P_{1/2}$ transition and 2×10^{12} atoms inside the cavity mode, the output laser power of Rb four-level quantum system active optical clock can reach 0.7 mW for $\Gamma_c = 100\Gamma_{35} = 1.29$ GHz. The quantum-limited linewidth can reach 0.7 Hz. The stability of light shift can be smaller than 0.18 mHz with the Rabi frequency of pumping laser 2.64×10^7 s $^{-1}$. Other alkali metals like potassium and cesium are also suitable for four-level quantum system active optical clock. An experimental configuration to realize active optical frequency standards based on Rb four-level quantum system is also given.

The authors thank Shengnan Zhang, Zhichao Xu and Zhong Zhuang for helpful discussions. This work was supported by the National Natural Science Foundation of China (10874009 and 11074011).

- 1 Chen J B. Active optical clock. *Chin Sci Bull*, 2009, 54: 348–352
- 2 Chen J B, Chen X Z. Optical lattice laser. In: *Proceedings of International Frequency Control Symposium*, 2005 Aug 29–31, Vancouver, Washington DC: IEEE, 2005. 608–610
- 3 Wang Y Q. Optical clocks based on stimulated emission radiation. *Chin Sci Bull*, 2009, 54: 347
- 4 Zhuang W, Yu D S, Chen J B. Optical clock based on quantum emitters. In: *Proceedings of International Frequency Control Symposium*, 2006 June 5–7, Florida, Washington DC: IEEE, 2006. 277–280
- 5 Zhuang W, Chen J B. Beyond one-second laser coherence via active optical atomic clock. In: *Proceedings of 20th European Frequency and Time Forum*, 2006 Mar 27–30, Braunschweig, Germany, 2006. 373–375
- 6 Zhuang W, Yu D S, Chen Z H, et al. Proposed active optical frequency standards based on magneto-optical trap trapped atoms. In: *Proceedings of European Frequency and Time Forum and International Frequency Control Symposium*, 2007 May 29–June 1, Geneva, Washington DC: IEEE, 2007. 96–99

- 7 Yu D S, Chen J. Laser theory with finite atom-field interacting time. *Phys Rev A*, 2008, 78: 013846
- 8 Chen J B. Active optical clock. In: *Proceedings of the 7th Frequency Standards and Metrology Symposium*, 2008 Oct 5–11, California, Washington DC: IEEE, 2008. 525–531
- 9 Meiser D, Ye J, Carlson D R, et al. Prospects for a millihertz-linewidth laser. *Phys Rev Lett*, 2009, 102: 163601
- 10 Meiser D, Holland M J. Steady-state superradiance with alkaline-earth-metal atoms. *Phys Rev A*, 2010, 81: 033847
- 11 Xie X P, Zhuang W, Chen J B. Adiabatic passage based on the Calcium active optical clock. *Chin Phys Lett*, 2010, 27: 074202
- 12 Zhuang W, Chen J B. Progress of active optical frequency standard based on thermal Ca atomic beam. In: *Proceeding of International Frequency Control Symposium*, 2010 June 2–4, California, Washington DC: IEEE, 2010. 222–223
- 13 Zhuang W, Chen J B. Feasibility of extreme ultraviolet active optical clock. *Chin Phys Lett*, 2011, 28: 080601
- 14 Zhuang W, Yu D S, Liu Z W, et al. Multi-threshold second-order phase transition in laser. *Chin Sci Bull*, 2011, 56: 3812–3816
- 15 Sterr U, Lisdat C. Millihertz-linewidth lasers: A sharper laser. *Nat Phys*, 2009, 5: 382–383
- 16 Qi R, Yu X L, Li Z B, et al. Non-Abelian Josephson effect between two $F = 2$ spinor Bose-Einstein condensates in double optical traps. *Phys Rev Lett*, 2009, 102: 185301
- 17 Ji A C, Sun Q, Xie X C, et al. Josephson Effect for Photons in two weakly Linked microcavities. *Phys Rev Lett*, 2009, 102: 023602
- 18 Ji A C, Liu W M, Song J L, et al. Dynamical creation of fractionalized vortices and vortex lattices. *Phys Rev Lett*, 2008, 101: 010402
- 19 Kuppens S J M, van Exter M P, Woerdman J P. Quantum-limited linewidth of a bad-cavity laser. *Phys Rev Lett*, 1994, 72: 3815–3818
- 20 An K, Feld M S. Semiclassical four-level single-atom laser. *Phys Rev A*, 1997, 56: 1662–1665
- 21 An K. Semiclassical theory of the many-atom microlaser. *J Korean Phys Soc*, 2003, 42: 505–517
- 22 Kessler T, Hagemann C, Grebin C, et al. A sub-40 mHz linewidth laser based on a silicon single-crystal optical cavity. 2011, arXiv: 1112.3854v1

Open Access This article is distributed under the terms of the Creative Commons Attribution License which permits any use, distribution, and reproduction in any medium, provided the original author(s) and source are credited.